Distributed Quasi-Dynamic State Estimation Incorporating Distributed Energy Resources

Boqi Xie[1], *Student Member, IEEE,* A. P. Sakis Meliopoulos[1], *Fellow, IEEE*
Chiyang Zhong[1], *Student Member, IEEE,* Yu Liu[2], *Member, IEEE*
Liangyi Sun[1], *Student Member, IEEE,* and Jiahao Xie[1], *Student Member, IEEE*
1. School of Electrical and Computer Engineering, Georgia Institute of Technology, Atlanta, Georgia 30332-0250, USA
2. School of Information Science and Technology, ShanghaiTech University, Shanghai, 201210, China
Email: bxie34@gatech.edu

***Abstract*—Deployment of distributed energy resources (DERs) introduces more dynamics to the distribution system, and brings system operators more challenges in monitoring and controlling the distribution system. These challenges can be addressed by developing methods for real time extraction of the operating state and model of the system, that is advanced state estimators for distribution systems with high penetration of DERs. This paper presents an object-oriented Distributed Quasi-Dynamic State Estimator (DQDSE) that employs three-phase detailed models and enables data from sensors to be streamed and used by the DQDSE. Based on three-phase detailed quasi-dynamic models that track slow dynamics (e.g., controls of power electronics, electromechanical transients of motors, etc.), DQDSE forms network measurement model by using network-wise measurements, performs quasi-dynamic state estimation, and provides the best estimate of the distribution system states. The proposed DQDSE has the following advantages: (1) detailed modeling approach ensures accurate results even when accommodating unbalanced and asymmetric systems; (2) the measurement set of DQDSE contains measurements from sensors as well as other measurement types to increase redundancy; (3) the distributed architecture of DQDSE enables fast data processing. The paper presents the method via an illustrative example that substantiates the effectiveness of DQDSE.**

***Index Terms*—distributed quasi-dynamic state estimation, distributed energy resources, object-oriented, three-phase detailed model**

I. Introduction

The distribution system is becoming more sophisticated than before with the distributed energy resources (DERs) being installed at a rapid pace. The DERs (including solar photovoltaic, wind turbines, energy storage, combined heat and power or cogeneration systems, etc.) create opportunities for operators to manage the load/voltage profile, improve power quality and resiliency, and help meet green energy goals [1]-[2]. However, the increasing number of DERs penetrated in the distribution system also brings a series of challenges [3]. One of them is the constantly changing operating states of the system, which generates problems for the operator to monitor and control the distribution system. In order to monitor the distribution system more accurately, a distribution system state estimator is required. It should be able to constantly provide the operating points of the distribution system and the validated data to distribution management system (DMS) for further applications (e.g., optimal control, etc.).

However, present conventional state estimator operating in the transmission level is architected in a centralized manner, i.e., all the data obtained from intelligent electronic devices (IEDs) are processed in a control center. In addition, the models employed for state estimation are simplified system models (e.g., positive sequence network by assuming balanced and symmetric system) [4]-[6]. Since the distribution system is in a distributed architecture with unbalanced and asymmetric characteristics, the conventional state estimator is not applicable and the state estimator for distribution system is in need.

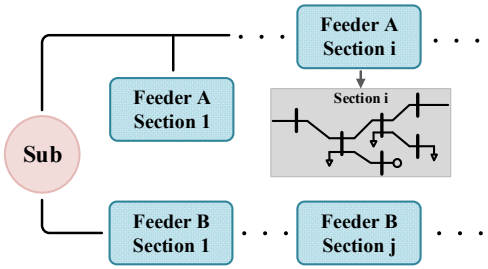

Figure 1: Partitioned Sections in Distribution System

Many efforts have been done to develop state estimators for distribution systems, and the Distributed Quasi-Dynamic State Estimator (DQDSE) is one of the solutions [7]-[9]. DQDSE employs Quasi-Dynamic State Estimation (QDSE), which uses phasor measurements and considers slow dynamics in the system such as electromechanical transients of rotating motors and controls of electronic devices. DQDSE is suitable for the distribution system for the following reasons: 1) DQDSE adopts three-phase detailed models to accommodate unbalanced/asymmetric system and outputs

This work is partially supported by the Department of Energy and Sandia National Laboratories. Their support is greatly appreciated.

978-1-5386-7138-2/18/$31.00 ©2018 IEEE

accurate results. 2) As shown in Fig. 1, the distribution system is arbitrarily partitioned into several sections, each having a DQDSE, which performs QDSE by using the measurements collected only in the corresponding section. This feature requires at least one GPS-synchronized IED in this section [10], and enables the data processed in a fast execution rate while still maintains the accuracy of the output. 3) DQDSE not only uses the actual measurements obtained from IEDs, but also creates additional measurements based on the device properties and system topology to increase the observability of the distribution system.

This paper introduces a fully object-oriented modeling approach to describe all the devices including DERs in the distribution system, and the state estimation technique that seamlessly accommodates the object-oriented models. The rest of the paper is organized as follows. Section II describes the fully object-oriented quasi-dynamic domain three-phase detailed modeling approach as the infrastructure of the DQDSE. Section III presents the object-oriented construction of the network measurement model and the algorithm of dynamic state estimation. Section IV demonstrates the results using an example section in a distribution system. Section V concludes the effectiveness of the DQDSE.

II. Object-Oriented Quasi-Dynamic Domain Three-Phase Detailed Device Modeling Approach

The object-oriented high-fidelity device modeling for the devices in the distribution system is the infrastructure of DQDSE. In this section, we introduce the modeling approach starting from the physically-based model referred to as the compact device model, which is a set of equations describing the physical and mathematical properties of the device. Since the compact model contains differential terms reflecting dynamics, the analytical solution is hard to obtain. Thus, we quadratize the equations and apply quadratic integration to the compact device model to eliminate the differential terms. The end result is an object-oriented interoperable model in a standardized syntax, and it is called the State and Control Algebraic Quadratic Companion Form (SCAQCF). The dynamic state estimation algorithm introduced in Section III works directly on these SCAQCF models without any other inputs (autonomous operation). To illustrate the detailed modeling approach, we select an average model of a DC-AC IGBT converter with a P-Q controller as an example.

A. Compact Device Model

A compact device model contains the equations that directly reflect the physical circuit of the device. As shown in Figure 2, the model equations for the converter are given by:

$$I_{AD} = \left(V_{AD} - V_{KD} - E_{DC}\right)/2r \quad (1)$$

$$I_{KD} = \left(-V_{AD} + V_{KD} + E_{DC}\right)/2r \quad (2)$$

$$\tilde{I}_a = \left(\tilde{V}_a - \tilde{E}_a\right)/j\omega L_s \quad (3)$$

$$\tilde{I}_b = \left(\tilde{V}_b - \tilde{E}_b\right)/j\omega L_s \quad (4)$$

$$\tilde{I}_c = \left(\tilde{V}_c - \tilde{E}_c\right)/j\omega L_s \quad (5)$$

$$0 = E_{DC} I_{AD} - P_{ac} \quad (6)$$

$$0 = \tilde{E}_a \exp\left(-j\,2\pi/3\right) - \tilde{E}_b \quad (7)$$

$$0 = \tilde{E}_a \exp\left(j\,2\pi/3\right) - \tilde{E}_c \quad (8)$$

$$0 = \mathrm{Re}\left(\tilde{V}_a \tilde{I}_a^* + \tilde{V}_b \tilde{I}_b^* + \tilde{V}_c \tilde{I}_c^*\right) + P_{ac} \quad (9)$$

$$0 = \mathrm{Im}\left(\tilde{V}_a \tilde{I}_a^* + \tilde{V}_b \tilde{I}_b^* + \tilde{V}_c \tilde{I}_c^*\right) + Q_{ac} \quad (10)$$

$$0 = -K_{P1}\, dP_{ac}/dt + K_{I1}\left(P_{ref} - P_{ac}\right) - d\sin\alpha/dt \quad (11)$$

$$0 = -K_{P2}\, dQ_{ac}/dt + K_{I2}\left(Q_{ref} - Q_{ac}\right) - dm/dt \quad (12)$$

$$0 = mE_{DC}\tilde{V}_a \Big/ \left(2\sqrt{2}\left|\tilde{V}_a\right|\right) - \tilde{E}_a \exp\left(-j\alpha\right) \quad (13)$$

where r is the equivalent resistance at the DC side, L_s is the equivalent inductance at the AC side, P_{ac} and Q_{ac} are the output active and reactive power of the converter at the AC side, P_{ref} and Q_{ref} are the reference active and reactive power outputs, m is the modulation index, and α is the phase shift between $\tilde{E}_a$ and $\tilde{V}_a$. Note that phasors are used in the compact device model.

The states of this model are V_{AD}, V_{KD}, $\tilde{V}_a$, $\tilde{V}_b$, $\tilde{V}_c$, E_{DC}, $\tilde{E}_a$, $\tilde{E}_b$, $\tilde{E}_c$, P_{ac}, Q_{ac}, m, and α. The control variables of this model are P_{ref} and Q_{ref}. Equations (11) and (12) indicate that the P-Q control of the converter is achieved by two PI controllers [11].

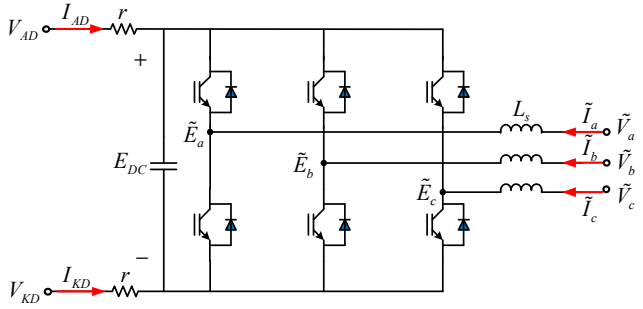

Figure 2: Circuit Diagram of DC-AC Converter

B. SCAQCF Device Model

To derive the SCAQCF device model, we first split the compact model into real and imaginary parts and quadratize them by introducing new states so that the device model only consists of linear and quadratic parts as shown in (14) and (15):

$$\begin{bmatrix} \mathbf{I(x,u)} \\ \mathbf{0} \end{bmatrix} = \mathbf{Y_{x1}x} + \mathbf{Y_{u1}u} + \mathbf{D_{x1}}\frac{d\mathbf{x}}{dt} + \mathbf{C_1} \quad (14)$$

$$\mathbf{0} = \mathbf{Y_{x2}x} + \mathbf{Y_{u2}u} + \begin{Bmatrix} \vdots \\ \mathbf{x}^{\mathrm{T}}\mathbf{F}_{\mathbf{x2}}^{\mathbf{i}}\mathbf{x} \\ \vdots \end{Bmatrix} + \begin{Bmatrix} \vdots \\ \mathbf{u}^{\mathrm{T}}\mathbf{F}_{\mathbf{u2}}^{\mathbf{i}}\mathbf{u} \\ \vdots \end{Bmatrix} + \begin{Bmatrix} \vdots \\ \mathbf{u}^{\mathrm{T}}\mathbf{F}_{\mathbf{ux2}}^{\mathbf{i}}\mathbf{x} \\ \vdots \end{Bmatrix} + \mathbf{C_2} \quad (15)$$

where $\mathbf{I(x,u)}$ is the terminal current vector, $\mathbf{x}$ is the state variable vector at time t, $\mathbf{u}$ is the control variable vector at time t, $\mathbf{Y_{x1}}$ and $\mathbf{Y_{x2}}$ are linear coefficient matrices associated

with states, $\mathbf{Y_{u1}}$ and $\mathbf{Y_{u2}}$ are linear coefficient matrices associated with controls, $\mathbf{D_{x1}}$ is the coefficient matrix of differential terms associated with states, $\mathbf{F^i_{x2}}$, $\mathbf{F^i_{u2}}$ and $\mathbf{F^i_{ux2}}$ denote quadratic terms, and $\mathbf{C_1}$, $\mathbf{C_2}$ are constant vectors.

Assuming the modeling time step of the above equation set is h, the next step is to apply quadratic integration with time step 2h [12] on (14) to eliminate the differential terms. The final expression (SCAQCF) is shown in (16). Notice that all the entries in the matrices are real values.

$$\begin{bmatrix}\mathbf{I(x,u)}\\ \mathbf{0}\end{bmatrix}=\mathbf{Y_x x}+\mathbf{Y_u u}+\begin{Bmatrix}\vdots\\ \mathbf{x}^{\mathrm{T}}\mathbf{F^i_x x}\\ \vdots\end{Bmatrix}+\begin{Bmatrix}\vdots\\ \mathbf{u}^{\mathrm{T}}\mathbf{F^i_u u}\\ \vdots\end{Bmatrix}+\begin{Bmatrix}\vdots\\ \mathbf{u}^{\mathrm{T}}\mathbf{F^i_{ux} x}\\ \vdots\end{Bmatrix}+\mathbf{B}, \quad (16)$$

$$\mathbf{B}=\mathbf{N_x x}(t-2h)+\mathbf{N_u u}(t-2h)+\mathbf{MI}(t-2h)+\mathbf{C}$$

where $\mathbf{x}=\begin{bmatrix}\mathbf{x}(t) & \mathbf{x}(t-h)\end{bmatrix}^T$, $\mathbf{u}=\begin{bmatrix}\mathbf{u}(t) & \mathbf{u}(t-h)\end{bmatrix}^T$,

$$\mathbf{Y_x}=\begin{bmatrix}\frac{2}{h}\mathbf{D_{x1}}+\mathbf{Y_{x1}} & -\frac{4}{h}\mathbf{D_{x1}}\\ \mathbf{Y_{x2}} & \mathbf{0}\\ \frac{1}{4h}\mathbf{D_{x1}} & \frac{1}{h}\mathbf{D_{x1}}+\mathbf{Y_{x1}}\\ \mathbf{0} & \mathbf{Y_{x2}}\end{bmatrix},\ \mathbf{Y_u}=\begin{bmatrix}\mathbf{Y_{u1}} & \mathbf{0}\\ \mathbf{Y_{u2}} & \mathbf{0}\\ \mathbf{0} & \mathbf{Y_{u1}}\\ \mathbf{0} & \mathbf{Y_{u2}}\end{bmatrix},\ \mathbf{F_x}=\begin{bmatrix}\mathbf{0} & \mathbf{0}\\ \mathbf{F_{x2}} & \mathbf{0}\\ \mathbf{0} & \mathbf{0}\\ \mathbf{0} & \mathbf{F_{x2}}\end{bmatrix},$$

$$\mathbf{F_u}=\begin{bmatrix}\mathbf{0} & \mathbf{0}\\ \mathbf{F_{u2}} & \mathbf{0}\\ \mathbf{0} & \mathbf{0}\\ \mathbf{0} & \mathbf{F_{u2}}\end{bmatrix},\ \mathbf{F_{ux}}=\begin{bmatrix}\mathbf{0} & \mathbf{0}\\ \mathbf{F_{ux2}} & \mathbf{0}\\ \mathbf{0} & \mathbf{0}\\ \mathbf{0} & \mathbf{F_{ux2}}\end{bmatrix},\ \mathbf{N_x}=\begin{bmatrix}-\mathbf{Y_{x1}}+\frac{2}{h}\mathbf{D_{x1}}\\ \mathbf{0}\\ \frac{1}{2}\mathbf{Y_{x1}}-\frac{5}{4h}\mathbf{D_{x1}}\\ \mathbf{0}\end{bmatrix},$$

$$\mathbf{N_u}=\begin{bmatrix}-\mathbf{Y_{u1}}\\ \mathbf{0}\\ \frac{1}{2}\mathbf{Y_{u1}}\\ \mathbf{0}\end{bmatrix},\ \mathbf{M}=\begin{bmatrix}\mathbf{I}\\ \mathbf{0}\\ -\frac{1}{2}\mathbf{I}\\ \mathbf{0}\end{bmatrix},\ \mathbf{C}=\begin{bmatrix}\mathbf{0}\\ \mathbf{C_2}\\ \frac{3}{2}\mathbf{C_1}\\ \mathbf{C_2}\end{bmatrix}.$$

III. Measurement Model and Distributed Dynamic State Estimation

This section introduces the computational procedure that enables data from sensors to be streamed and used by the DQDSE. With increasing deployment of smart meters and other grid sensors in the distribution system, the amount of available measurements is growing. These measurements as well as the other measurements proposed in this section construct the DQDSE measurement set that improves the observability of the distribution system. Given the measurement set and all the device models from a certain distribution section, the DQDSE first creates the measurement model at the device level, and then uses the network formation technique to create the measurement model at the network level. The dynamic state estimation works directly on the network level measurement model.

A. Measurement Set and Device-Level Measurement Model

In this subsection, we propose a measurement set to increase the redundancy and further improve the accuracy of the DQDSE: a) actual measurements: voltage or current measurements obtained from IEDs or other smart meters, b) derived measurements: derived from actual measurements based on the distribution system topology, c) virtual measurements: equations with zero value defined by physical or mathematical laws (e.g., KCL, device internal equations, etc.), and d) pseudo measurements: quantities that are approximately known (e.g., zero value of neutral phase voltage at normal operation, etc.).

If an actual voltage measurement is collected, the DQDSE simply formulates the measurement equation in a linear combination of the state variables of the measured device, i.e.,

$$z(t)=A\mathbf{x}(t)+\eta, \quad (17)$$

where $z(t)$ is the measurement, A is the linear coefficient matrix, $\mathbf{x}(t)$ is the device state vector, and η is the noise error introduced by the IED. If an actual current measurement is collected, the DQDSE forms the measurement model by obtaining the corresponding through equation from the device SCAQCF model, i.e.,

$$z(t)=Y_{zx}\mathbf{x}+Y_{zu}\mathbf{u}+\begin{Bmatrix}\vdots\\ \mathbf{x}^T F^i_{zx}\mathbf{x}\\ \vdots\end{Bmatrix}+\begin{Bmatrix}\vdots\\ \mathbf{u}^T F^i_{zu}\mathbf{u}\\ \vdots\end{Bmatrix}+\begin{Bmatrix}\vdots\\ \mathbf{u}^T F^i_{zux}\mathbf{x}\\ \vdots\end{Bmatrix}+B_z+\eta$$

$$B_z=N_{zx}\mathbf{x}(t-2h)+N_{zu}\mathbf{u}(t-2h)+M_z i(t-2h)+K_z \quad (18)$$

B. Construction of Network-Level Measurement Model

Once the device-level measurement model is formed, the DQDSE creates the network measurement model by performing two tasks: 1) Create the network SCAQCF model of the selected distribution system section and the network actual measurement model; 2) create the network derived, virtual and pseudo measurement models based on the network SCAQCF model and the topology.

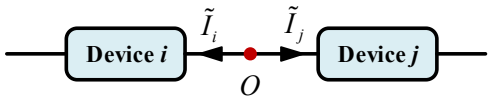

Figure 3: Illustration of Derived Measurements

The first task is to form the network SCAQCF model that has the same syntax as the device SCAQCF model. This is achieved by creating the mapping lists (states, equations, and controls) from devices to the network. The network actual measurement model is also created according to these mapping lists. The second task is to create the network-level derived, virtual and pseudo measurement models. The network derived measurements are created by derivations from actual measurements based on the network topology. For instance, as shown in Fig. 3, device *i* and *j* are connected at node *O* with available current phasor measurement $\tilde{I}_i$. Since no other devices are connected at point *O*, the current flowing into device *j* is simply derived as $z=\tilde{I}_j+\eta=-\tilde{I}_i+\eta$, and it is a derived measurement. The

network virtual measurements are obtained from the network SCAQCF model, which provides the network KCL equations at the common nodes and the device internal equations. The network pseudo measurements are created by searching the neutral and ground nodes in the network, and setting their voltage values to zero with a relatively high measurement error.

By combining all these measurements together, we form the network measurement model, which has a similar syntax as the network SCAQCF model:

$$\begin{aligned}\mathbf{z} &= h(\mathbf{x},\mathbf{u}) + \boldsymbol{\eta} \\ &= \mathbf{Y}_{xz}\mathbf{x} + \mathbf{Y}_{uz}\mathbf{u} + \begin{Bmatrix}\vdots\\ \mathbf{x}^{\mathrm{T}}\mathbf{F}_{xz}^{\mathbf{i}}\mathbf{x}\\ \vdots\end{Bmatrix} + \begin{Bmatrix}\vdots\\ \mathbf{u}^{\mathrm{T}}\mathbf{F}_{uz}^{\mathbf{i}}\mathbf{u}\\ \vdots\end{Bmatrix} + \begin{Bmatrix}\vdots\\ \mathbf{u}^{\mathrm{T}}\mathbf{F}_{uxz}^{\mathbf{i}}\mathbf{x}\\ \vdots\end{Bmatrix} + \mathbf{B}_{\mathbf{z}} + \boldsymbol{\eta} \\ \mathbf{B}_{\mathbf{z}} &= \mathbf{N}_{xz}\mathbf{x}(t-2h) + \mathbf{N}_{uz}\mathbf{u}(t-2h) + \mathbf{M}_{\mathbf{z}}\mathbf{I}(t-2h) + \mathbf{K}_{\mathbf{z}}\end{aligned} \quad (19)$$

where $\mathbf{x} = \begin{bmatrix}\mathbf{x}(t) & \mathbf{x}(t-h)\end{bmatrix}^T$, $\mathbf{u} = \begin{bmatrix}\mathbf{u}(t) & \mathbf{u}(t-h)\end{bmatrix}^T$, $\mathbf{z}$ is the measurement vector of the system, $\mathbf{Y}_{xz}$ is the linear coefficient matrix associated with state vector $\mathbf{x}$, $\mathbf{Y}_{uz}$ is the linear coefficient matrix associated with control vector $\mathbf{u}$, $\mathbf{F}_{xz}^{\mathbf{i}}$ is the quadratic coefficient matrix associated with states, $\mathbf{F}_{uz}^{\mathbf{i}}$ is the quadratic coefficient matrix associated with controls, $\mathbf{F}_{uxz}^{\mathbf{i}}$ is the quadratic coefficient matrix associated with the product of states and controls, $\mathbf{B}_{\mathbf{z}}$ is the history-dependent vector, and $\boldsymbol{\eta}$ is the vector of measurement errors.

Meanwhile, the standard deviation is introduced for each measurement to represent the measurement error. For actual measurements, the standard deviations are the meter errors of the corresponding IEDs. For the derived measurements, their standard deviations are the same as the ones of actual measurements where they are derived from. Since the virtual measurements are the equations obeying mathematical or physical laws, their errors are much smaller compared to those of actual measurements. Therefore, we set their standard deviations to be a relatively low value (e.g., 0.001 p.u.). Similarly, as we only know the expected value of pseudo measurements, they have larger errors than the actual measurements. Thus, we set their standard deviation to be a relatively high value (e.g., 0.1 p.u.).

C. Dynamic State Estimation Algorithm

The weighted least square method is used in the state estimation algorithm [13], and the objective function for this problem is:

$$\textit{Minimize} \quad J = \left(\mathbf{z} - h(\mathbf{x},\mathbf{u})\right)^{\mathrm{T}} \mathbf{W} \left(\mathbf{z} - h(\mathbf{x},\mathbf{u})\right), \quad (20)$$

where $\mathbf{W}$ is the weight matrix with the weights defined as the inverse of the squared standard deviations δ_i for each measurement:

$$\mathbf{W} = \mathrm{diag}\left\{1/\delta_1^2, 1/\delta_2^2, \cdots, 1/\delta_n^2\right\}. \quad (21)$$

Then we substitute the control vector $\mathbf{u}$ in $h(\mathbf{x},\mathbf{u})$ with actual values from DMS, yielding $h(\mathbf{x})$, and apply linearization technique on it at point $\mathbf{x}^{\nu}$ by assuming that $\mathbf{x}^{\nu}$ is very close to the optimal solution. The linearization error is:

$$\mathbf{r} = h(\mathbf{x}^{\nu}) + \partial h(\mathbf{x})/\partial \mathbf{x}\Big|_{\mathbf{x}=\mathbf{x}^{\nu}} \left(\mathbf{x} - \mathbf{x}^{\nu}\right) - \mathbf{z} = \mathbf{H}\mathbf{x} - \mathbf{z}', \quad (22)$$

where $\mathbf{H} = \partial h(\mathbf{x})/\partial \mathbf{x}\Big|_{\mathbf{x}=\mathbf{x}^{\nu}}$, and $\mathbf{z}' = -h(\mathbf{x}^{\nu}) + \mathbf{H}\mathbf{x}^{\nu} + \mathbf{z}$.

Now the problem is expressed as:

$$\textit{Minimize} \quad J = \left(\mathbf{H}\mathbf{x} - \mathbf{z}'\right)^{\mathrm{T}} \mathbf{W} \left(\mathbf{H}\mathbf{x} - \mathbf{z}'\right). \quad (23)$$

The optimal solution is obtained by:

$$dJ/d\mathbf{x} = 0. \quad (24)$$

Thus, the solution is achieved by the following iterative equation:

$$\mathbf{x}^{\nu+1} = \left(\mathbf{H}^{\mathrm{T}}\mathbf{W}\mathbf{H}\right)^{-1} \mathbf{H}^{\mathrm{T}}\mathbf{W}\mathbf{z}' = \mathbf{x}^{\nu} - \left(\mathbf{H}^{\mathrm{T}}\mathbf{W}\mathbf{H}\right)^{-1} \mathbf{H}^{\mathrm{T}}\mathbf{W}\left(h\left(\mathbf{x}^{\nu}\right) - \mathbf{z}\right). \quad (25)$$

Notice that the algorithm performs state estimation using two consecutive measurements (time t and t-h). In addition, the past history terms $\mathbf{x}(t-2h)$ and $\mathbf{I}(t-2h)$ are updated by $\mathbf{x}(t)$ and $\mathbf{I}(t)$ at each time step.

Once the solution is computed, we apply the chi-square test to it. The chi-square test provides a mathematical method of evaluating whether the measurements fit the system model. The procedure is as follows:

First, the chi-square is computed as:

$$\xi = \sum_i \left(\frac{h_i(\mathbf{x}) - z_i}{\delta_i}\right)^2. \quad (26)$$

Next, the confidence level is obtained:

$$\mathrm{P} = 1 - \Pr(\xi, \upsilon), \quad (27)$$

where υ is the degree of freedom, which is the difference between the number of measurements and states. The confidence level computed exhibits the consistency between the measurements and the system model. A high value (e.g., 100%) indicates the measurements matching the system model, and the estimated states and measurements are trustworthy. A low value (e.g., 0%) implies the occurrence of some bad data or hidden failures in the system.

IV. Illustrative Results

This section illustrates that the proposed DQDSE is able to accurately estimate the states of an overall section of a distribution system. The example section of a distribution system for demonstration is shown in Fig. 4. This section consists of several distribution system elements (including a DER) as well as six IEDs. We simulated the measurements collected by these IEDs and store them into a COMTRADE file for state estimation purposes.

A. System Configuration

This example section consists of two three-phase distribution lines, two single-phase distribution lines, two single-phase transformers with center-tap, two balanced loads at secondary bus, one three-phase two-winding transformer, one DC/AC converter, and one energy storage system

(battery). The major parameters of these devices are listed in Table 1, and the total number of states in this section is 81. In addition, six IEDs are installed in this section. IED 1 collects the voltage, current, and state of charge (SOC) measurements of the battery. IED 2 monitors the voltage and current measurements at both terminals of the three-phase transformer. IEDs 3 and 4 measure the voltages and currents of the two single-phase transformers with center-tap. IEDs 5 and 6 monitor the voltages and currents at the interfaces of this section. IED placements and their measurement channels are also depicted in Fig. 4.

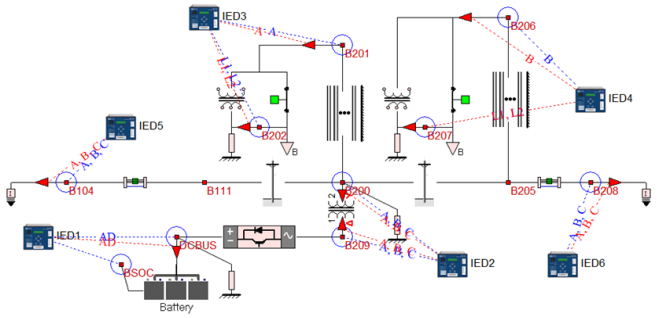

Figure 4: Example Section in a Distribution System

Table 1: Major Parameters of Devices in the Example Section

Distribution Line			
Device Name	Bus Name	Rated Voltage (kV)	Length (mile)
3Φ Line 1	B111, B200	13.8	1.05
3Φ Line 2	B200, B205	13.8	0.70
1Φ Line 1	B200, B201	13.8	0.3
1Φ Line 2	B205, B206	13.8	0.5
Transformer			
Device Name	Bus Name	Rated Voltage (kV)	Connection Type
3Φ XMFR	B200, B209	13.8/0.4	Wye/Delta
1Φ XMFR	B201, B202	7.96/0.24	N/A
1Φ XMFR	B206, B207	7.96/0.24	N/A
Load			
Device Name	Bus Name	Real Power (kW)	Reactive Power (kVar)
Load 1	B202	40.0	5.0
Load 2	B207	40.0	5.0
Converter			
Device Name	Bus Name	Rated Voltage (kV)	P-Q Control (kW/kVar)
DC/AC Converter	B200, B209	0.4/0.8	80.0/10.0
Battery			
Device Name	Bus Name	Rated Voltage (kV)	Capacity (kCoulombs)
Battery	DCBUS	0.8	1350

In this example, we have 18 voltage phasor measurements, 18 current phasor measurements, 1 DC voltage measurement, 1 DC current measurement and 1 SOC measurement. Since DQDSE divides each phasor measurement into real and imaginary parts, we have 75 actual measurements in total. Furthermore, the DQDSE automatically creates the derived, virtual and pseudo measurements: 1) 15 derived measurements (current measurements from B111 to B200, B202 to B201, B207 to B206, and the DC current flowing into the converter), 2) 64 virtual measurements (36 obeying KCL equations at B200, B201, B202, B206, B207, B209, and DCBUS, and 28 being internal equations in the converter and transformers), and 3) 18 pseudo measurements (neutral voltage being close to zero). In summary, we have 172 measurements, and we set the standard deviation of actual, derived, virtual and pseudo measurements to be 0.01 p.u., 0.01 p.u., 0.001 p.u., and 0.1 p.u, respectively.

B. Simulation Results

We created a 20-second event with some load changes outside this section to demonstrate the effectiveness of the proposed DQDSE. The DQDSE uses section-wise measurements and estimates the states of the whole section. Since the generated data are very large in size and the number of pages is limited, we depict the state estimation results by some specific data. Figs. 5-8 present the voltage and current actual and estimated phasor measurements at both sides of the three-phase transformer. These figures indicate that the estimated measurements track the measurements from IED 2 accurately.

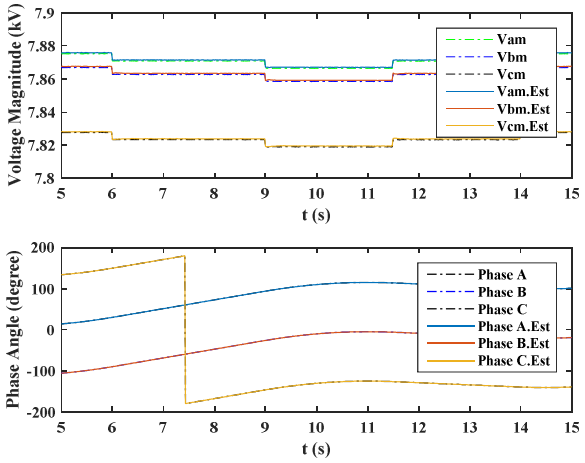

Figure 5: Actual and Estimated Voltage Phasor Measurements at B200

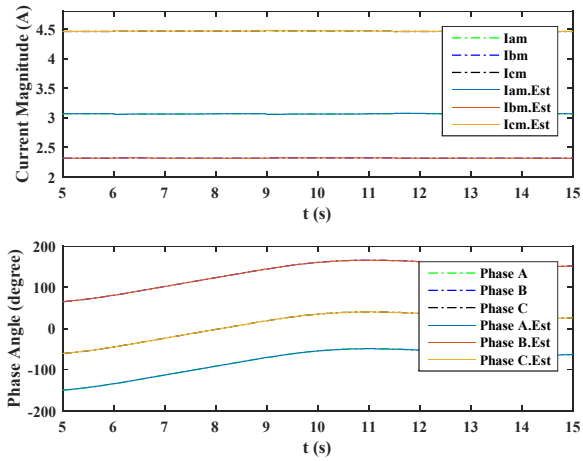

Figure 6: Actual and Estimated Current Phasor Measurements from B200 to B209

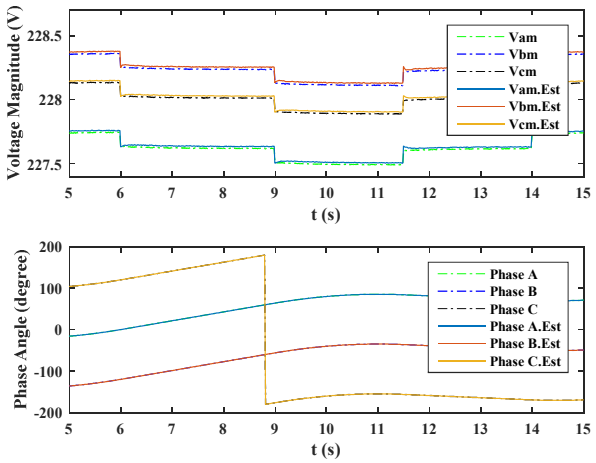

Figure 7: Actual and Estimated Voltage Phasor Measurements at B209

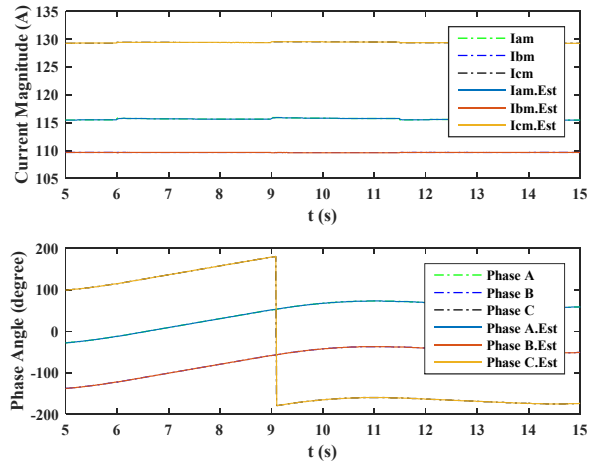

Figure 8: Actual and Estimated Current Phasor Measurements from B209 to B200

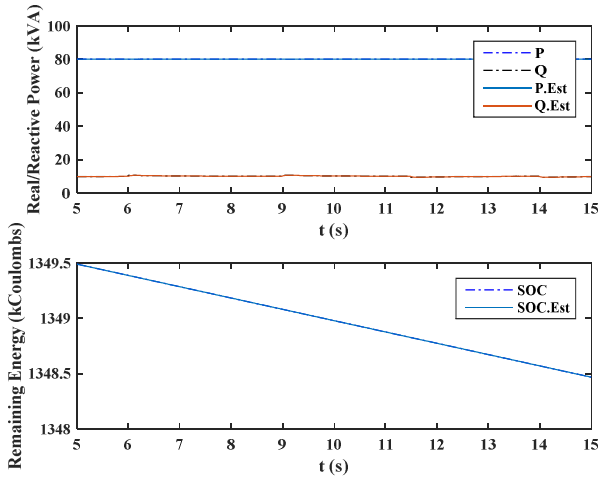

Figure 9: Actual and Estimated Power Output from Converter and SOC of Battery

Fig. 9 exhibits the actual/estimated real and reactive power output from the converter as well as the actual/estimated state of charge (SOC) of the battery. This figure indicates that the converter constantly controls the real and reactive power at the desired values and the estimated real and reactive power keep tracking the actual values. The actual/estimated SOC value in this figure also proves that the estimated measurements match perfectly with the actual ones. Notice that the SOC actual measurement (dash-dot line) is completely covered by the estimated SOC measurement (solid line). Furthermore, the confidence level of the whole section remains at 100% during the event, which indicates a strong consistency between the measurements and the system model, i.e., the measurements obtained from the IEDs and the system model of this section are validated.

V. Conclusions

This paper presents an object-oriented distributed quasi-dynamic state estimator for distribution systems with high penetration of DERs. The DQDSE has the following features: 1) three-phase detailed modeling approach ensures accurate results; 2) use of additional derived, virtual and pseudo measurements to enhance the observability of the distribution system; 3) The dynamic state estimation algorithm seamlessly accommodates the detailed models and measurement models without any other inputs. Moreover, the trustworthy output information from the state estimator can be used for further applications that require real-time model and system operating conditions, such as voltage regulation, distribution system optimal power flow, etc.

References

[1] A Review of Distributed Energy Resources, NYISO, Sept. 2014

[2] Jiayi Huang, Jiang Chuanwen, and Xu Rong. "A review on distributed energy resources and MicroGrid." *Renewable and Sustainable Energy Reviews* 12, no. 9 (2008): 2472-2483.

[3] J. Driesen and R. Belmans, "Distributed generation: challenges and possible solutions," *2006 IEEE Power Engineering Society General Meeting*, Montreal, Que., 2006, pp. 1-8.

[4] A. Monticelli. *State estimation in electric power systems: a generalized approach*. Vol. 507. Springer Science & Business Media, 1999.

[5] A. Abur, and A. G. Exposito. *Power system state estimation: theory and implementation*. CRC press, 2004.

[6] A. P. S. Meliopoulos and G. K. Stefopoulos, "Characterization of state estimation biases," *Probabilistic Methods Applied to Power Systems, International Conference*, Ames, IA, 2004, pp. 600-607.

[7] S. A. P. Meliopoulos, "Legacy SE to distributed dynamic state estimators: evolution and experience," *IEEE Power & Energy Society General Meeting*, Denver, CO, 2015, pp. 1-5.

[8] A. P. Meliopoulos, E. Polymeneas, Zhenyu Tan, Renke Huang, and Dongbo Zhao, "Advanced Distribution Management System", *IEEE Transactions on Smart Grid*, Vol 4, Issue 4, pp 2109-2117, 2013.

[9] Renke Huang, George Cokkinides, Clinton Hendrington, and A. P. Meliopoulos, "Distribution System Distributed Quasi-Dynamic State Estimator", *IEEE Transactions on Smart Grid*, Volume 7, No. 6, pp 2761-2770, November 2016

[10] B. Xie, A. P. S. Meliopoulos, Y. Liu and L. Sun, "Distributed quasi-dynamic state estimation with both GPS-synchronized and non-synchronized data," *2017 North American Power Symposium (NAPS)*, Morgantown, WV, 2017, pp. 1-6.

[11] S. Adhikari, F. Li and H. Li, "P-Q and P-V Control of Photovoltaic Generators in Distribution Systems," in *IEEE Transactions on Smart Grid*, vol. 6, no. 6, pp. 2929-2941, Nov. 2015.

[12] Meliopoulos, A. P., George J. Cokkinides, and George K. Stefopoulos. "Quadratic integration method." In *Proceedings of the 2005 International Power System Transients Conference (IPST 2005)*, pp. 19-23. 2005.

[13] L. Sun, A. P. S. Meliopoulos, Y. Liu and B. Xie, "Dynamic state estimation based synchronous generator model calibration using PMU data," *2017 IEEE Power & Energy Society General Meeting*, Chicago, IL, 2017, pp. 1-5.